

Evaluation of TELSEM² using observed sea ice emissivities up to 340 GHz in preparation for the Ice Cloud Imager (ICI)



Nils Risse¹, M. Mech¹, C. Prigent², G. Spreen³, J. Rückert³, A. Walbröl¹, and S. Crewell¹

¹Institute for Geophysics and Meteorology, University of Cologne; ²Laboratoire d'Etudes du Rayonnement et de la Matière en Astrophysique et Atmosphères, Observatoire de Paris, CNRS; ³Institute of Environmental Physics, University of Bremen

1. Introduction

- Use of passive MW observations from satellites for atmospheric retrievals over sea ice is limited by uncertain sea ice emissivity.
- TELSEM² provides first-guess land and sea ice emissivity estimate anchored to a satellite climatology up to 90 GHz and extrapolated to sub-mm frequencies [1].
- So far, TELSEM² was not evaluated over sea ice above 200 GHz.

- Utilize four airborne and one ship-based campaign
- Derive emissivity directly from observations
- Investigate various sea ice conditions

2. Field data

- Five campaigns were conducted with varying MW instrumentation.

Campaign	Platform	Radiometers	Viewing angle
ACLOUD	Aircraft ¹	MiRAC-P, MiRAC-A	0°, 25°
AFLUX	Aircraft ¹	MiRAC-P, MiRAC-A	0°, 25°
MOSAIC-ACA	Aircraft ¹	HATPRO, MiRAC-A	0°, 25°
HALO-AC3	Aircraft ¹²	HATPRO ¹ , MiRAC-A ¹ , HAMP ²	0°, 25°, 0°
WALSEMA	Ship ³	MiRAC-P, HATPRO	53°/10-70°

¹Polar 5 (AWI), ²HALO (DLR), ³R/V Polarstern (AWI)

- Ancillary measurements by IR radiometers and dropsondes/radiosondes.

MiRAC-P: 6×183.31 (V-pol), 243, 340 GHz (H-pol) [2]

MiRAC-A: 89 GHz (H-pol) [2]

HATPRO: 7 K-, and 7 V-band frequency channels (H-pol)

HAMP: like HATPRO plus 90, 4×118.75, 7×183.31 GHz

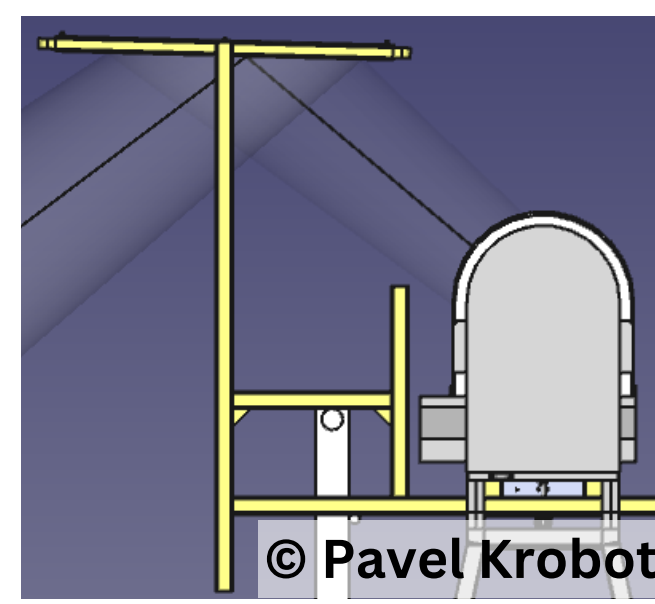


Fig. 1: MWR setup onboard R/V Polarstern.

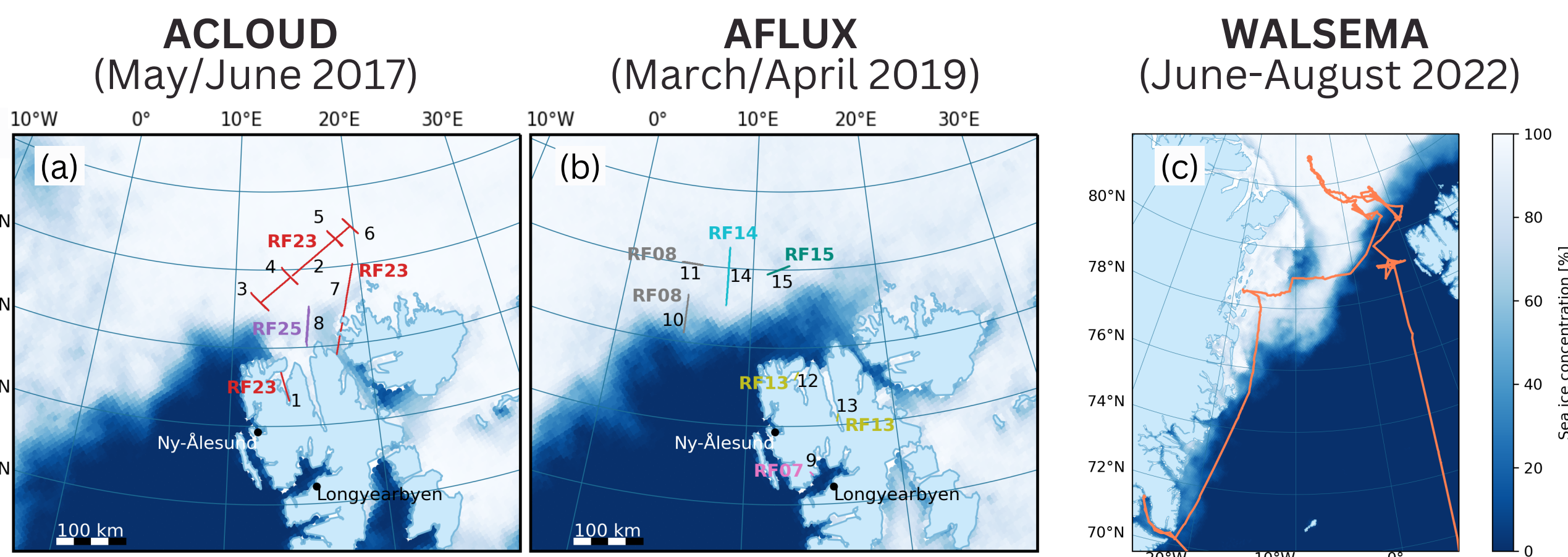


Fig. 2: Map of clear-sky flight segments used for the sea ice emissivity calculation during the two airborne missions: (a) ACLOUD and (b) AFLUX. (c) Shows the ship track during the recent WALSEMA mission. The sea ice concentration derived from AMSR2 (Univ. of Bremen) is shown as background.

3. Emissivity calculation

- From observed TB and PAMTRA[3] simulation of atmospheric emission.
- Surface reflection assumed either Lambertian (L) or specular (S).
- Limitation: Similar T_s and $T_a \downarrow$ and low transmissivity lead to high uncertainties, especially at 340 GHz in summer (Fig. 3).

$$T_b = e \cdot T_s \cdot t(0, h) + (1-e) \cdot T_a \cdot t(0, h) + T_a t$$

$$\Leftrightarrow e = \frac{T_b - T_b(e=0)}{T_b(e=1) - T_b(e=0)} \quad [4,5]$$

e : sea ice emissivity
 T_b : observed brightness temperature [K]
 T_s : IR sea ice (skin) temperature [K]
 h : flight altitude [m]
 T_a : atmospheric emission [K]
 t : atmospheric transmissivity

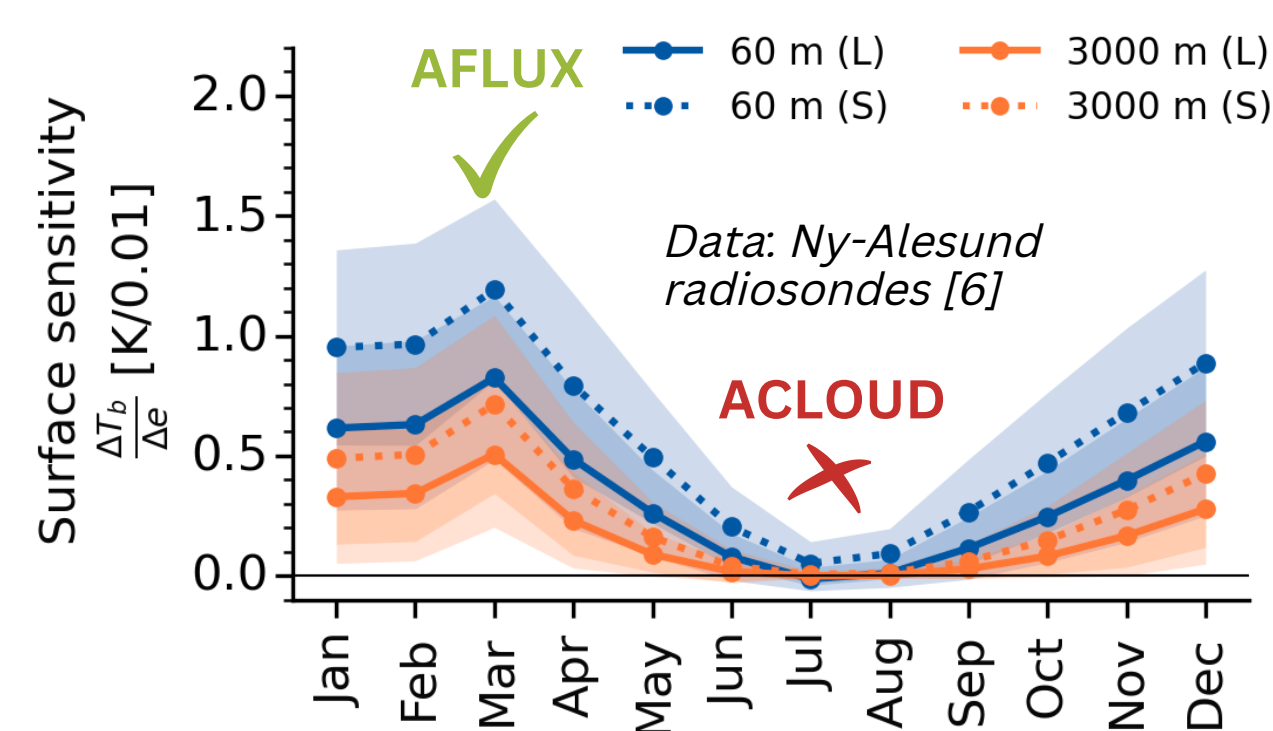


Fig. 3: Seasonal limitation of the emissivity calculation from observed TB at 340 GHz (Constraint: $T_s \leq 0^\circ\text{C}$).

4. Evaluation of campaign-based sea ice emissivity

- Sea ice emissivities at nadir show high variability depending on the sea ice structure (see upper panel in Fig. 4)
 - Compact ice floes: ($e=0.7-0.8$), snow-free leads: ($e=0.8-0.9$)
- Spectral emissivity variation above 183 GHz is limited as assumed in extrapolation of TELSEM².

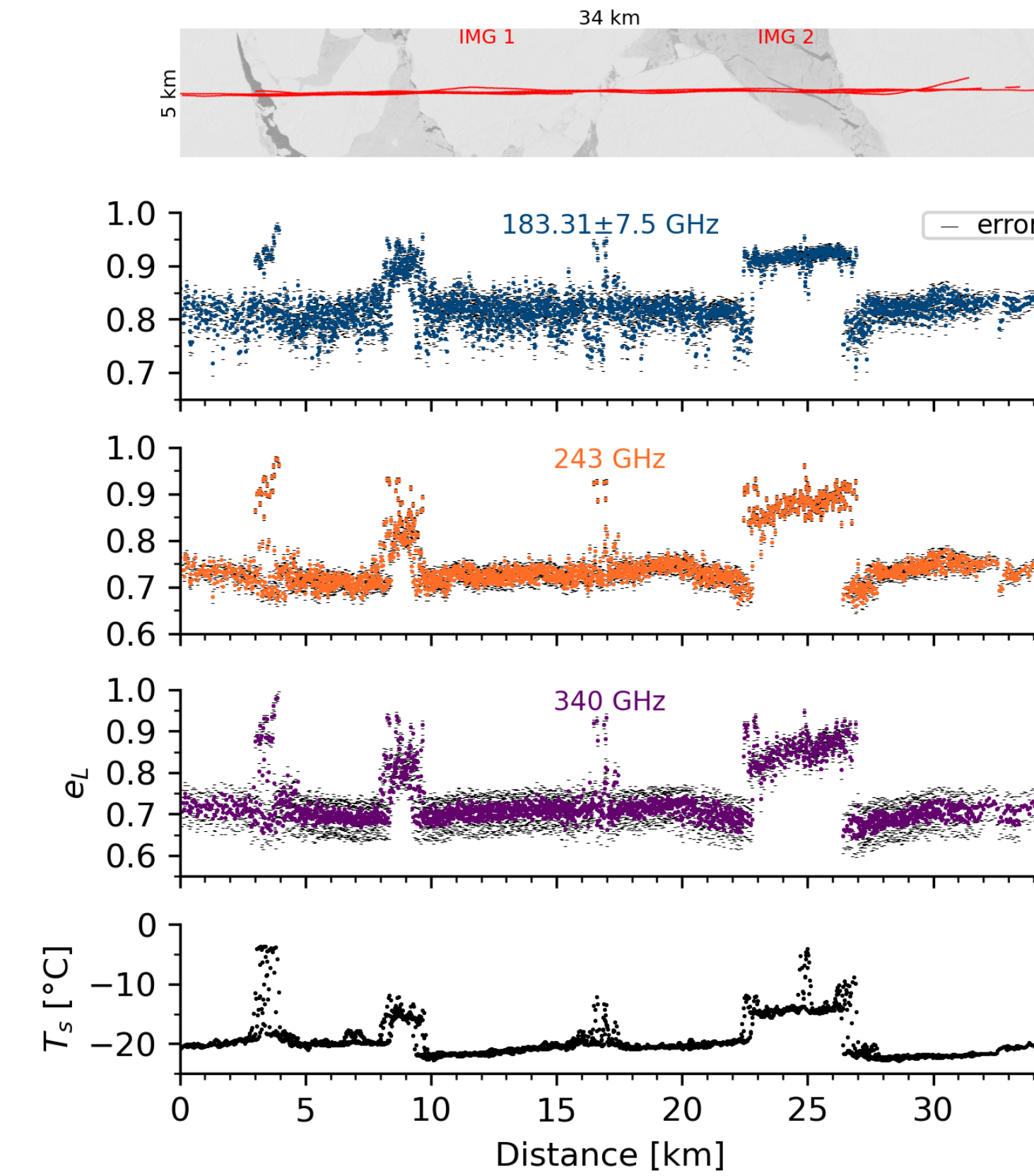


Fig. 4: Emissivity variation over two sea ice types in the marginal ice zone between 183 and 340 GHz. (Leg 15)

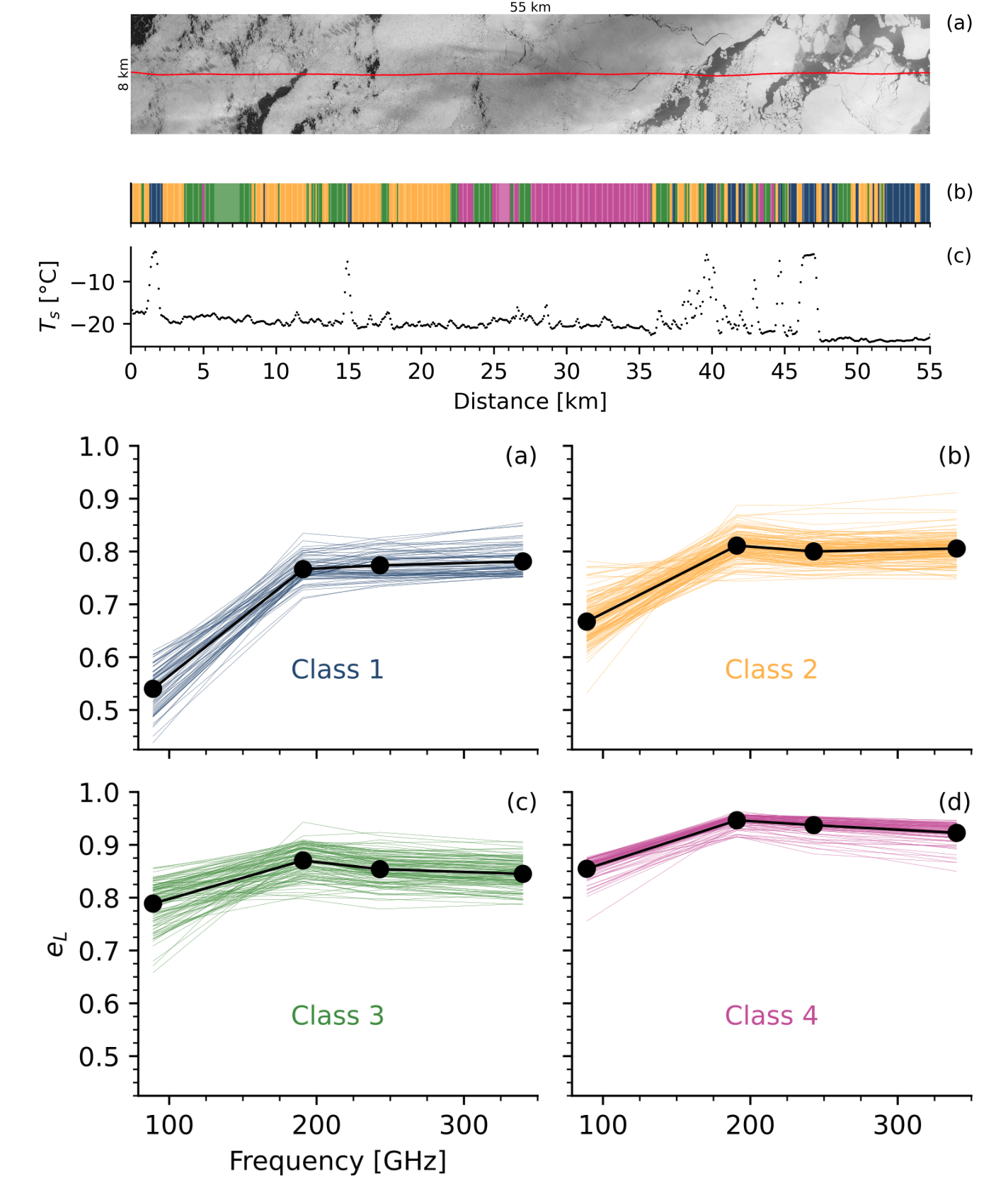


Fig. 5: Spatial variation of emissivity spectra classified using K-Means between 89 and 340 GHz. (Leg 10)

5. Difference between TELSEM² and observations

- Good agreement during ACLOUD under specular reflection, except for 89 GHz, but high uncertainty at 340 GHz (Fig. 3).
- Consistently higher TELSEM² emissivities during AFLUX, where airborne estimates are accurate up to 340 GHz
- Frequency extrapolation does not explain the observed difference

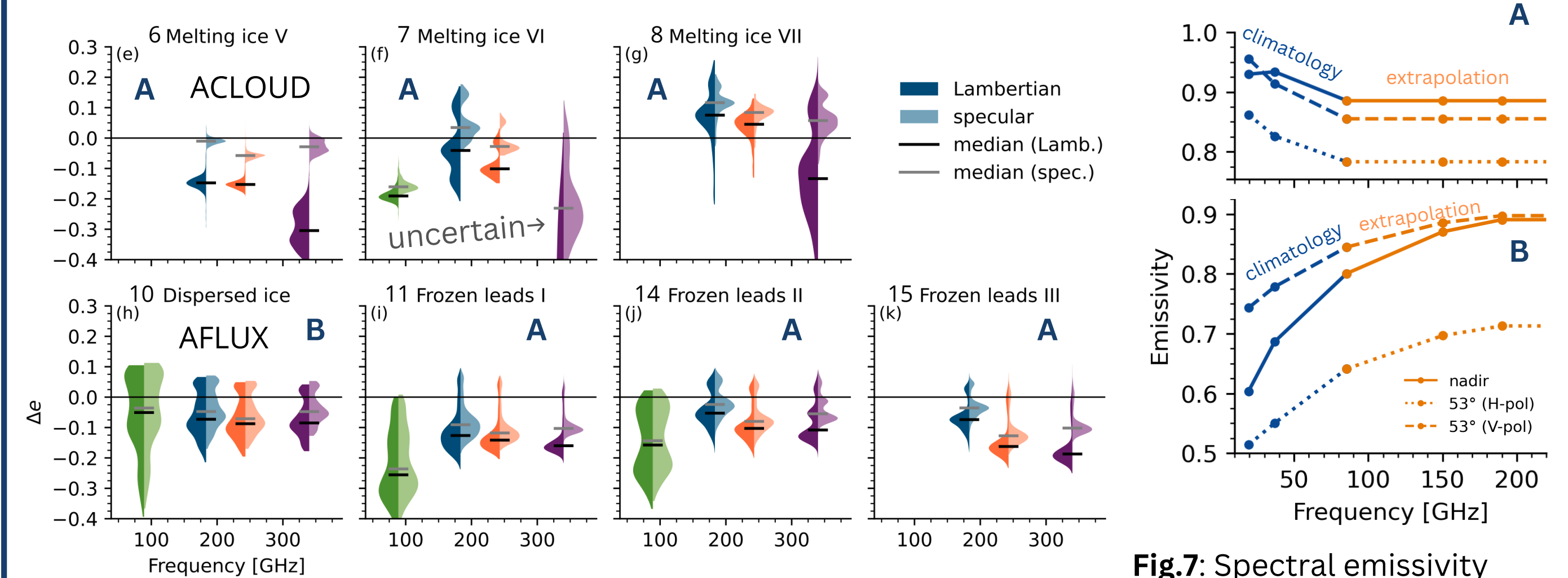


Fig. 6: Distributions of the difference between airborne emissivities and TELSEM² ($e(\text{MiRAC}) - (\text{TELSEM}^2)$) along the flight track for all legs north of Svalbard. The number indicates the location of the flight leg in Fig. 2.

Fig. 7: Spectral emissivity extrapolation of TELSEM² for regions with mostly multi-year ice (top) and the marginal ice zone (bottom).

6. Conclusions and outlook

- Airborne-derived emissivities show clear dependence on sea ice properties such as snow cover, causing high spatial emissivity variations.
- Assumption of constant emissivities above 183 GHz is reasonable.
- Consistent offsets between TELSEM² and the airborne estimates occur, which require further investigation.
- The angular emissivity variation might be one explanation, which will be studied from shipborne observations.
- Co-locations with MW satellite instruments will be investigated.

References:

- [1] Wang, D., Prigent, C., Kilic, L., Fox, S., Harlow, C., Jimenez, C., ... Karbou, F. (2017). Surface emissivity at microwaves to millimeter waves over polar regions: Parameterization and evaluation with aircraft experiments. *Journal of Atmospheric and Oceanic Technology*, 34(5), 1039-1059. doi: 10.1175/JTECH-D-16-0188.1
- [2] Mech, M., Kliesch, L.-L., Anhäuser, A., Rose, T., Kollias, P., & Crewell, S. (2019). Microwave radar/radiometer for arctic clouds (MiRAC): first insights from the ACLOUD campaign. *Atmospheric Measurement Techniques*, 12(9), 5019-5037.
- [3] Mech, M., Maahn, M., Kneifel, S., Ori, D., Orlandi, E., Kollias, P., ... Crewell, S. (2020). PAMTRA 1.0: the Passive and Active Microwave radiative TRANSfer tool for simulating radiometer and radar measurements of the cloudy atmosphere. *Geoscientific Model Development*, 13(9), 4229-4251.
- [4] Prigent, C., Rossow, W. B., & Matthews, E. (1997). Microwave land surface emissivities estimated from SSM/I observations. *Journal of Geophysical Research*, 102, 21867-21890.
- [5] Mathew, N., Heygster, G., Melsheimer, C., & Kaleschke, L. (2008). Surface emissivity of arctic sea ice at AMSU window frequencies. *IEEE Transactions on Geoscience and Remote Sensing*, 46(8), 2298-2306.
- [6] Maturilli, M. (2020). High resolution radiosonde measurements from station Ny-Alesund (2017-04 et seq) [data set]. PANGAEA. Retrieved 2021-11-19, from https://doi.org/10.1594/PANGAEA.914973